Manuscript submitted to
AIMS' Journals
Volume **X**, Number **0X**, XX **200X**

Website: http://AIMsciences.org
pp. **X–XX**

SHOOTING AND NUMERICAL CONTINUATION METHODS FOR COMPUTING TIME-MINIMAL AND ENERGY-MINIMAL TRAJECTORIES IN THE EARTH-MOON SYSTEM USING LOW PROPULSION.

Gautier Picot

Mathematics Institute, Bourgogne University
9 avenue Savary
21078 Dijon, France

(Communicated by the associate editor name)

Abstract. In this article we describe the principle of computations of optimal transfers between quasi-Keplerian orbits in the Earth-Moon system using low-propulsion. The spacecraft's motion is modeled by the equations of the control restricted 3-body problem and we base our work on previous studies concerning the orbit transfer in the two-body problem where geometric and numeric methods were developped to compute optimal solutions. Using numerical simple shooting and continuation methods connected with fundamental results from control theory, as the Pontryagin Maximum Principle and the second order optimality conditions related to the concept of conjugate points, we compute time-minimal and energy-minimal trajectories between the geostationary initial orbit and a final circular one around the Moon, passing through the neighborhood of the libration point L_1. Our computations give simple trajectories, obtained by referring to numerical values of the SMART-1 mission.

1. **Introduction.** The aim of this article is to study the optimal orbit transfer between quasi-Keplerian orbits in the Earth-Moon system when low propulsion is applied. This study is in particular motivated by the recent mission SMART-1 of the European Space Agency, see [26, 27], which has already been investigated in depth, using for example simple feedback laws [7] or the transcription method [4]. Our model is the circular restricted 3-body problem [24] that has provided the framework to numerous dynamical systems studies about space mission design in the solar system, see notably [19, 21]. The physical issue is to maximize the final mass of the spacecraft but, as a first step, we restrict our analysis to the time-minimal control problem and the so-called energy minimization problem, see also [8, 16, 17] for complementary results, for two reasons. First of all, the first problem will provide an estimate about the time transfer. Second, the energy minimization problem is a L^2-regularization of the mass maximization problem which is a non smooth L^1-problem. This regularization is known to be an important step in the analysis, see [18]. Our work is based on previous works concerning the orbit transfer between

2000 *Mathematics Subject Classification.* Primary: 49K15, 49M05; Secondary: 70F07.

Key words and phrases. Geometric control theory, numerical analysis method, 3-body problem, Earth-Moon transfer, time minimization problem, energy minimization problem.

The author is supported by supported by CNRS (contract no. 37244) and Conseil Régional de Bourgogne (contrat no. 079201PP02454515).

Keplerian orbit in the two-body problem with low propulsion, see [15, 18], where geometric and numeric techniques were developed to compute the optimal solutions. They are based on the so-called indirect method in optimal control where optimal solutions are found among a set of extremal curves, solutions of the Pontryagin's Maximum Principle [25]. This led to compute the solution using a shooting method where the solution is computed using a Newton method. In this framework, a continuation method is used to solve the delicate problem of finding a precise enough initial solution, see [2].

The first section of this article presents the main results from geometric control theory connected to our analysis with adapted numerical codes developed to compute the solutions. First of all, the maximum principle is only a necessary optimality condition. In order to get necessary sufficient optimality conditions (under generic assumptions) one must define the concept of conjugate point, which was already introduced in the standard literature of calculus of variations [6] and can be generalized in optimal control, see for instance [1, 13]. If the Hamiltonian optimal dynamics is described by a smooth Hamiltonian vector field $\overrightarrow{H}$, conjugate points are the image of the singularities of the exponential mapping : $\exp_{q(0)} : p(0) \longrightarrow \Pi_q(\exp_{t_f}(\overrightarrow{H})(q(0), p(0)))$ where $\Pi_q : (q, p) \longrightarrow q$ is the standard projection. Such a point can be numerically computed using the Cotcot code described in [9]. Besides, an important remark, in view of the use of the (smooth) continuation method in optimal control, is to observe that the shooting equation is precisely to find $p(0)$ such that $\exp_{q(0)}(p(0)) = q_1$ where q_1 is the terminal condition and the derivative can be generated using the variational equation of $\overrightarrow{H}$. This will lead to convergence results for the smooth continuation method in optimal control, related to estimates of conjugate points [14].

The second section is devoted to present the system which is deduced from the standard circular restricted model where the two primaries are fixed in a rotating frame, see [24, 22, 30]. Up to a normalization the system can be written in the Hamiltonian form

$$\dot{z} = \overrightarrow{H_0}(z) + u_1 \overrightarrow{H_1}(z) + u_2 \overrightarrow{H_2}(z)$$

where $z = (q, p) \in \mathbb{R}^4$ and $\overrightarrow{H_0}$ is the Hamiltonian vector field corresponding to the the drift

$$H_0(z) = \frac{1}{2}(p_1^2 + p_2^2) + p_1 q_2 - p_2 q_1 - \frac{1-\mu}{\varrho_1} - \frac{\mu}{\varrho_2},$$

q being the position of the spacecraft, ϱ_1 representing the distance to the Earth with mass $1-\mu$ located at $(-\mu, 0)$ and ϱ_2 the distance to the Moon with mass μ and located at $(1-\mu, 0)$, while $\mu \simeq 0.012153$ is a small parameter. The Hamiltonian lifts associated with the control correspond to the functions

$$H_i(z) = -q_i, \text{ for } i = 1,\ 2$$

and $\parallel u \parallel$ is bounded by ϵ.

The third section deals with the time-minimal Earth-Moon transfer problem. In that case, the norm of an extremal control is constant outside a set of measure zero, see [10]. A preliminary study will focus on the Earth-L_1 transfer, which provides an approximation of the first phase of the Earth-Moon transfer. Using our geometric analysis, a locally minimizing extremal is numerically computed using a continuation method on the control bound ϵ. Actually, the convergence of the simple shooting method is easily obtained with large thrust, the transfer time being short, and provides a starting point to the continuation method, see [12]. This first study naturally leads to the analysis of time-minimal Earth-Moon trajectories. In addition, we propose a time-minimal transfer strategy towards the Lagrange point L_4, in order to compare, from the topological point of view, extremal trajectories associated with different targets. Finally, we proceed to a numerical verification of the relation of comparison between the first conjugate times in the normal and abnormal cases, see [13]. .

The fourth section is devoted to the energy minimization of the Earth-Moon transfer. The parameter μ is small and this remark was used by Poincaré to study the dynamics of the free motion described by $\overrightarrow{H_0}$, by making a deformation of the case $\mu = 0$ which corresponds to the Kepler problem in rotating coordinates, see [23]. Inspired by this approach we propose a simple solution to the energy-minimal Earth-Moon transfer using low propulsion, after having investigated the Earth-L_1 transfer case.

2. Numerical methods in optimal control.

2.1. Optimal control problem.

Let M and U be two smooth manifolds of respective dimensions n and m. Consider the control system

$$\dot{q}(t) = f(q(t), u(t)) \tag{1}$$

where $f : M \times U \longrightarrow TM$ is smooth and u is a bounded measurable function defined on $[0, t(u)[\subset \mathbb{R}^+$ and valued in U. Let M_0 and M_1 be two subsets of M.

Definition 2.1. Let be $q_0 \in M$. One calls *trajectory associated with the control* u the solution $q(t, q_0, u)$ of 1 starting from q_0 at $t = 0$. For the sake of simplicity, such a trajectory can be denoted $q(t)$. A control u is called an *admissible control on* $[0, t_f]$, with $t_f < t(u)$, if its associated trajectory satisfies $q_0 \in M_0$ and $q(t_f) \in M_1$. One denotes by $\mathcal{U}_{t_f}$ the set of these admissible controls and defines the *cost* of q by

$$C(t_f, u) = \int_0^{t_f} f^0(q(t), u(t))dt \tag{2}$$

where $f^0 : M \times U \longrightarrow \mathbb{R}$ is smooth. Solving the optimal control problem consists in determining an admissible control u such that C is minimized.

Definition 2.2. Let be $q_0 \in M$ and $t_f > 0$. The *end-point mapping* is defined by

$$\begin{aligned} E_{q_0,t_f} : \mathcal{U}_{t_f} &\longrightarrow M \\ u &\longrightarrow q(q_0, t_f, u). \end{aligned} \tag{3}$$

If $\mathcal{U}_{t_f}$ is endowed with the L^∞ topology then the end-point mapping is smooth. Let us remark that, for every $\epsilon > 0$, an admissible control u can be smoothly extended to $[0, t_f + \epsilon]$, provided the control is left continuous at t_f.

Definition 2.3. Consider two distinct cases.

– If the final time is fixed, q is said to be *locally optimal* in L^∞ topology if it is optimal in a neighborhood of u in L^∞ topology.
– If the final time is not fixed and the control is left continuous at t_f, $q(.)$ is said to be *locally optimal* in L^∞ topology if for each neighborhood V of u in $L^\infty([0, t_f + \epsilon], U)$, for each η such that $|\eta| \leq \epsilon$ and for each control $v \in V$ which satisfies $E(q_0, t_f + \eta, v) = E(q_0, t_f, u)$ then $C(t_f + \eta, v) \geq C(t_f, u)$.

2.2. **The Pontryagin's Maximum Principle.** Consider the control system 1 and the cost 2. The Pontryagin's Maximum Principle [25] asserts that if the control $u \in \mathcal{U}_{t_f}$ is optimal then there exists p^0 a nonpositive real and p an absolutely continuous mapping on $[0,t_f]$ such that $p(t) \in T^*_{q(t)}M$, $(p^0,p) \neq (0,0)$ and, almost everywhere on $[0,t_f]$, there holds

$$\dot{q} = \frac{\partial H}{\partial p}(q,p,p^0,u),\ \dot{p} = -\frac{\partial H}{\partial q}(q,p,p^0,u), \tag{4}$$

where H is defined by

$$\begin{aligned} H : T^*M \times \mathbb{R}^*_- \times U &\longrightarrow \mathbb{R} \\ (q,p,p^0,u) &\longrightarrow p^0 f^0(q,u) + < p, f(q,u) > . \end{aligned}$$

Moreover, the optimal control satisfies the maximization condition

$$H(q(t),p(t),p^0,u(t)) = \max_{v\in U} H(q(t),p(t),p^0,v) \tag{5}$$

almost everywhere on $[0,t_f]$. If t_f is not fixed, there holds

$$\max_{v\in U} H(q(t),p(t),p^0,v) = 0 \tag{6}$$

for every $t \in [0,t_f]$. Finally, if M_0 (resp. M_1) is a regular submanifold of M, the transversality condition is satisfied

$$p(0) \perp T_{q(0)}M_0 \quad (\text{resp.} \quad p(t_f) \perp T_{q(t_f)}M_1). \tag{7}$$

Definition 2.4. One calls *pseudo-Hamiltonian* the mapping H and *costate* the function p. A solution (q,p,p^0,u) of equations 4 and 5 is called an *extremal*. If $p^0 = 0$, an extremal is said to be *abnormal*. Otherwise it is said to be *normal*.

Since the domain U is a manifold, restricting to a chart we may assume that, locally, $U = \mathbb{R}^m$ and the maximization condition leads to $\frac{\partial H}{\partial u} = 0$. Express the following assumption.

(**L**) (Strong Legendre condition) The quadratic form $\frac{\partial^2 H}{\partial u^2}$ is negative definite along the reference extremal.

From the implicit function theorem, one deduces that extremal controls are smooth functions $u_r(t) = u_r(q(t),p(t))$ in a neighborhood of u.

Definition 2.5. One defines the *true Hamiltonian*, denoted H_r, by

$$H_r(q,p) = H(q,p,u_r(q,p)). \tag{8}$$

Then any extremal is solution of the Hamiltonian system

$$\dot{q} = \frac{\partial H_r}{\partial p}(q,p),\ \dot{p} = -\frac{\partial H_r}{\partial q}(q,p). \tag{9}$$

Denoting $z = (q,p)$, this system writes

$$\dot{z} = \overrightarrow{H_r}(z(t)). \tag{10}$$

2.3. **Second order optimality condition.** Let us briefly present the concept of geometric conjugate time which is related to a second order optimality condition, see [9] for the details. Consider a smooth manifold M of dimension n and denote $\Pi_q : T^*M \longrightarrow M$ the standard projection from the cotangent bundle T^*M on M. Let $\overrightarrow{H}$ be an Hamiltonian vector field on T^*M and $z(t) = (q(t), p(t))$ a trajectory of $\overrightarrow{H}$ defined on $[0, t_f]$ so that there holds $\dot{z}(t) = \overrightarrow{H}(z(t))$ for each $t \in [0, t_f]$.

Definition 2.6. The variational equation on $[0, t_f]$

$$\delta\dot{z}(t) = d\overrightarrow{H}(z(t)).\delta z(t) \tag{11}$$

is called the *Jacobi equation* along $z(.)$. One calls a *Jacobi field* a nontrivial solution $J(t)$ of the Jacobi equation along $z(.)$ and it is said to be *vertical* at the time t if $\mathrm{d}\Pi_q(z(t)).J(t) = 0$. A time t_c is said to be *geometrically conjugate* if there exists a Jacobi field vertical at 0 and t_c. In which case, $q(t_c)$ is said to be *conjugate* to $q(0)$.

Let us point out that, in local coordinates, one can write a Jacobi field $J(t) = (\delta q(t), \delta p(t))$. Then J is vertical at the time t whenever $\delta q(t) = 0$. When the final target is a regular submanifold $M_1 \subset M$, the notion of conjugate time is generalized as follows.

Definition 2.7. Denote $M_1^\perp = \{(q,p),\, q \in M_1, p \perp T_q M_1\}$. Then a time $t_{\mathrm{foc}} \in [0, T]$ is said to be a *focal time* if there exists a Jacobi field $J = (\delta q, \delta p)$ such that $\delta q(t_{foc}) = 0$ and $J(t_{foc})$ is tangent to $M_1^\perp$.

Definition 2.8. Let be $z_0 \in T^*M$. For each $t \in [0, t_f]$, one defines the *exponential mapping* by

$$\exp_t : z_0 \longrightarrow \Pi_q(z(t, z_0)) \tag{12}$$

where $z(t, z_0)$ is the trajectory of $\overrightarrow{H}$ satisfying $z(0, z_0) = z_0$.

Using local coordinates and setting $z_0 = (q_0, p_0) \in T^*M$, one writes $z(t, q_0, p_0) = (q(t, q_0, p_0), p(t, q_0, p_0))$. Setting $q_0 \in M$ as the initial condition, the exponential mapping writes $exp_{q_0,t}(p_0) = q(t, q_0, p_0)$. Let $\exp_t(\overrightarrow{H})$ be the flow of $\overrightarrow{H}$. The following proposition results from a geometrical interpretation of the Jacobi equation.

Proposition 1. *Let be $q_0 \in M$, $L_0 = T^*_{q_0}M$ and $L_t = exp_t(\overrightarrow{H})(L_0)$. Then L_t is a Lagrangian submanifold of T^*M whose tangent space is spanned by Jacobi fields starting from L_0. Moreover $q(t_c)$ is geometrically conjugate to q_0 if and only if exp_{q_0,t_c} is not an immersion at p_0.*

The following proposition, see [11], will be used to formulate the relevant generic assumptions.

Proposition 2. *An extremal control is a singularity of the end-point mapping when the set of admissible controls $\mathcal{U}$ is endowed with the L^∞-topology. Moreover, the adjoint vector $p(t)$ is orthogonal to the image of $D_u E_{q_0,t}$.*

The following assumptions is needed to derive second order optimality conditions in the normal case.

(**S**) (Strong regularity) On every subinterval of $[0, t_f]$, the control u is of corank 1.

As a result, one can enunciate the following crucial theorem which connects the notion of conjugate time and the local optimality of extremals, see [1, 13, 28].

Theorem 2.9. *Let t_c^1 be the first conjugate time along z. Under previous assumptions, the trajectory $q(.)$ is locally optimal on $[0, t_c^1)$ in L^∞ topology; if $t > t_c^1$ then $q(.)$ is not locally optimal on $[0, t]$.*

2.4. **Simple shooting method.** We previously stated that the maximization and strong Legendre conditions enable to write locally any extremal control under the form $u_r(t) = u_r(q(t), p(t))$, the extremal system becoming $\dot{z} = \overrightarrow{H_r}(z(t))$ where $z = (q, p)$.

Expressing boundary and transversality conditions by $R(z(0), z(t_f)) = 0$, the boundary values problem becomes

$$\left\{ \begin{array}{c} \dot{z} = \overrightarrow{H_r}(z(t)) \\ R(z(0), z(t_f)) = 0. \end{array} \right. \tag{13}$$

The initial condition q_0 is fixed which leads to the following definition.

Definition 2.10. Assume that the transfer time t_f is fixed. One calls *shooting function* the mapping E defined by

$$E : p_0 \longrightarrow R(z_0, z_{t_f}). \tag{14}$$

It is important to notice that whenever one considers an optimal control problem with a non-fixed transfer time, the corresponding shooting function applies on (t_f, p_0). Moreover, the condition $H_r = 0$ from the maximum principle provides one additional equation. Hence solving the boundary values system is equivalent to finding a zero of E, that is to say solving the so-called *shooting equation*. Since $u_r(q, p)$ is smooth, E is smooth and such a zero can be found using a Newton type algorithm, providing that one has a precise initial guess of it. The continuation method is appropriate to overcome this difficulty.

2.5. **Smooth continuation method.** Without loss of generality, one can assume that the final time t_f is fixed and the final condition is written $q_f = q_1$, the following results being adaptable to other cases. The smooth continuation method consists in considering the reduced Hamiltonian H_r as the element H_1 of a family $(H_\lambda)_{\lambda \in [0,1]}$ of smooth Hamiltonians. One thus builds up the one-parameter family of shooting functions defined by

$$E_\lambda(p_0) = exp^\lambda_{q_0, t_f}(p_0) - q_1. \tag{15}$$

Considering the normal case, the following theorem is deduced from the implicit function theorem, see [14].

Theorem 2.11. *For each λ the exponential mapping $exp^\lambda_{q_0}$ is of maximal rank if and only if the point $q_1 = exp^\lambda_{q_0, t_f}(p(0))$ is non-conjugate to q_0. Moreover, solutions of the parametrized shooting equation contain a smooth curve, which can be parametrized by λ and the derivative $E_\lambda^{'}$ can be computed integrating the Jacobi equation.*

For more details, in paticular about geometric considerations relative to this theorem, one can refer to [20]. The scheme of the smooth continuation method to compute solutions of the shooting equation is the following :

1. One determines the starting point p_0 of the continuation method using a simple shooting. Setting $\lambda = 0$, one computes the extremal $z(t)$ on $[0, t_f]$ starting from (q_0, p_0).

2. One chooses a discretization $0{=}\lambda_0$, $\lambda_1,\ldots,\lambda_N{=}1$ such that the shooting function is solved iteratively at λ_{i+1} from λ_i.
3. One builds up the finite sequence $p_0,\ldots, p_N$ with zeros of shooting functions $E_{\lambda_0},\ldots, E_{\lambda_N}$.

From theorem 2.11, a crucial point to guarantee the convergence of the smooth continuation method is to check the lack of conjugate points along each extremal z_λ on $[0, t_f]$, which must be iteratively performed.

2.6. **Numeric methods.** They are implemented in the COTCOT (Conditions of Order Two, COnjugate Times) whose aim is to provide the numerical tool :

- to integrate the smooth Hamiltonian vector field $\overrightarrow{H_n}$,
- to solve the associated shooting equation,
- to compute the corresponding Jacobi fields along the extremals,
- to evaluate the resulting conjugate points.

The code is written in Fortran language, while automatic differentiation provided by the software *Adifor* [5] is used to generate the Hamiltonian differential equation and the variational one. For the users the language is Matlab, see [10] for a precise description of the Cotcot code, with the underlying algorithms: *Netlib* Runge-Kutta one-step ODE integrator [29], *Netlib* HYBRD Newton solver. The conjugate point test consists in checking a rank condition which is based on two methods: evaluating zeros of a determinant or a SVD (Singular Value Decomposition). The continuation method will be included in the code which can be a simple discretization of the homotopy path, with a Newton method at each step or a numeric continuation of the path, using the implicit ODE, where the Newton method is used only at the first step to initialize the continuation and at the final step, to solve the final shooting equation with arbitrary accuracy.

3. The restricted 3-body problem.

3.1. **The circular restricted 3-body problem in Jacobi coordinates.** Recall the following representation of the Earth-Moon problem, see [24, 30]. In the rotating frame, the Earth which is the biggest primary planet with mass $1-\mu$ is located at $(-\mu, 0)$ while the Moon with mass μ, is located at $(1-\mu, 0)$ with the small parameter $\mu \simeq 0.012153$. We denote $z = x + iy$ the position of the spacecraft and $\varrho_1 = \sqrt{((x+\mu)^2 + y^2)}$, $\varrho_2 = \sqrt{((x-1+\mu)^2 + y^2)}$ are the distances to the primaries. The equation of motion takes the form

$$\ddot{z} + 2i\dot{z} - z = -(1-\mu)\frac{z+\mu}{\varrho_1^3} - \mu\frac{z-1+\mu}{\varrho_2^3} \tag{16}$$

which can be written

$$\begin{aligned} \ddot{x} - 2\dot{y} - x &= \frac{\partial V}{\partial x} \\ \ddot{y} + 2\dot{x} - y &= \frac{\partial V}{\partial y} \end{aligned} \tag{17}$$

where $-V$ is the potential of the system defined by $V = \frac{1-\mu}{\varrho_1} + \frac{\mu}{\varrho_2}$. The system can be written using Hamiltonian formalism setting

$$q_1 = x,\ q_2 = y,\ p_1 = \dot{x} - y,\ p_2 = \dot{y} + x$$

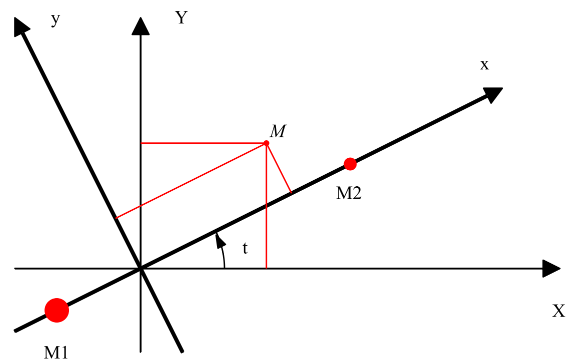

FIGURE 1. The rotating coordinates system (x, y) relatively to the inertial coordinates (X, Y).

and the Hamiltonian describing the motion takes the form

$$H_0(q_1, q_2, p_1, p_2) = \frac{1}{2}(p_1^2 + p_2^2) + p_1 q_2 - p_2 q_1 - \frac{1-\mu}{\varrho_1} - \frac{\mu}{\varrho_2}. \tag{18}$$

3.2. **Equilibrium points.** The equilibrium points of the problem are well known. They split in two different types :

– *Euler points.* They are the collinear points denoted L_1, L_2 and L_3 located on the line $y = 0$ defined by the primaries. For the Earth-Moon problem they are given by

$$x_1 \simeq 0.8369,\ x_2 \simeq 1.1557,\ x_3 \simeq -1.0051.$$

– *Lagrange points.* The two points L_4 and L_5 form with the two primaries an equilateral triangle.

Some important informations about stability of the equilibrium points are provided by the eigenvalues of the linearized system. The linearized matrix evaluated at points L_1, L_2 or L_3 admits two real eigenvalues, one being strictly positive and two imaginary ones. The collinear points are consequently non stable. In particular, the eigenvalues of the linearized matrix evaluated at L_1 with $\mu = 0.012153$ are ± 2.931837 and $\pm 2.334248i$. When it is evaluated at L_4 or L_5, the linearized matrix has two imaginary eigenvalues when $\mu < \mu_1 = \frac{1}{2}(1 - \frac{\sqrt{69}}{9})$. So in the Earth-Moon system, the points L_4 and L_5 are stable, according to the Arnold's stability theorem [3] since $\mu < \mu_1$.

3.3. **The control system.** The control system in the rotating frame is deduced from the previous model and can be written using the Hamiltonian formalism

$$\dot{z} = \overrightarrow{H}_0(z) + u_1 \overrightarrow{H}_1(z) + u_2 \overrightarrow{H}_2(z) \tag{19}$$

where $\overrightarrow{H}_0$ is the free motion and $\overrightarrow{H}_1$, $\overrightarrow{H}_2$ are the Hamiltonian vector fields corresponding to the functions $H_i = -q_i$ for $i = 1, 2$. As for the Kepler problem, see [15], the spacecraft mass variation may be modelled dividing u_i by $m(t)$ and considering the equation $\dot{m} = -\delta|u|$. This will not be taken into account and we will focus on both time-minimal transfer problem

$$\min_{u(.)\in B_{\mathbb{R}^2}(0,\epsilon)} \int_{t_0}^{t_f} dt \tag{20}$$

where ϵ is the maximum thrust allowed by spacecraft's engines and energy-minimal transfer problem

$$\min_{u(.)\in \mathbb{R}^2} \int_{t_0}^{t_f} u_1^2 + u_2^2 dt \tag{21}$$

when the transfer time t_f is fixed and the constraint on the control bound is relaxed. The first problem will provide an estimation of the Earth-Moon transfer time when low thrust is used. The energy minimization problem will give a starting point in order to perform a homotopy method relating the final spacecraft mass maximization problem and the energy minimization problem

$$\min_{u(.)} \int_0^{t_f} (\lambda|u|^2 + (1-\lambda)|u|)dt,\ \lambda \in [0,1].$$

4. **Time-minimal transfers in the Earth-Moon system.**

4.1. **Normal case.**

4.1.1. *Generalities on the normal case.* Let us recall fundamental results about time-minimal control problems. Consider a bi-input control system on $\mathbb{R}^n$

$$\dot{q} = F_0(q) + \epsilon \sum_{i=1}^{2} u_i F_i(q), \quad \epsilon > 0, \quad u_1^2 + u_2^2 \leq 1 \tag{22}$$

and the time-minimal problem 20. Then the pseudo-Hamiltonian from the maximum principle is

$$H(z,u) = p^0 + H_0(z) + \epsilon(u_1 H_1(z) + u_2 H_2(z)) \tag{23}$$

where $z = (q,p) \in T^*\mathbb{R}^n$ and $H_i(z) =< p, F_i(q) >,\ i = 0, \dots, 2$. The maximization condition implies that when $(H_1, H_2) \neq (0,0)$, the control u is given by

$$u_i = \frac{H_i}{\sqrt{H_1^2 + H_2^2}},\ i = 1,\ 2. \tag{24}$$

In the normal case $p^0 \neq 0$, one can normalize p^0 to -1 and so

$$H_r(z) = -1 + H_0(z) + \epsilon\sqrt{(H_1^2(z) + H_2^2(z))}. \tag{25}$$

Since the transfer time is not fixed, H_r is identically zero on $[0, t_f]$.

Definition 4.1. One calls *switching surface* the set

$$\Sigma = \{z \in T^*\mathbb{R}^n,\ H_1(z) = H_2(z) = 0\}.$$

One calls *point of order 0* an element $z \in T^*\mathbb{R}^n \backslash \Sigma$ and *point of order 1* an element $z \in \Sigma$ such that $(\dot{H}_1(z), \dot{H}_2(z)) \neq 0$.

In particular, an extremal control belongs to the unit circle $\mathbb{S}^1$ outside the switching surface. Consider the specific case $q \in \mathbb{R}^4$. Under specific conditions, we have the following result, see [10] for the complete proof.

Proposition 3. *At a point of order 1, the control u instantaneously rotates of an angle π i.e $u(t^+) = -u(t^-)$.*

The following proposition is a corollary of the above result.

Proposition 4. *Each normal time-minimal trajectory is a concatenation of a finite number of arcs of order 0 with π-singularities at junction points.*

As we will see in the section 4.1.3, the second order system of controlled equations of motion in the circular 3-body problem can be expressed as a bi-input system in $\mathbb{R}^4$ with $F_1 = \frac{\partial}{\partial q_3}$ and $F_2 = \frac{\partial}{\partial q_4}$. Conditions of the proposition 4 are consequently fulfilled, see [10], that allows to use a continuation method on the control bound to compute time-minimal Earth-Moon trajectories.

4.1.2. *Continuation method on the control bound.* Considering a bi-input control system on $\mathbb{R}^4$ satisfying some regularity properties, proposition 4 asserts that the control corresponding to a time-minimal trajectory has a constant norm outside a set of measure zero. Such regularity properties are satisfied regarding the orbital transfer control in the Kepler problem, justifying the numerical continuation method on the control bound, see [15] and [18]. We statued that the same justification holds in the case of the restricted 3-body problem and we use the numerical continuation method to compute time-minimal extremals with low-thrust.By choosing the parameter ϵ corresponding to a large enough value, the time transfer is short and the simple shooting method directly converges on a starting point of the continuation method. Mention that our numerical study results in computing only extremals of order 0. Consequently, the time minimal extremal control vectors we determined are continuous along the transfer time. However, it is clear that the simple shooting and the continuation method can be performed with extremals of order one, providing the use of an adaptive integration step. As a preliminary study, we will focus on the Earth-L_1 transfer which is a good representation of the first phase of the Earth-Moon transfer. By simplifying the final condition, we make the simple shooting and the numerical continuation easier. So we compute more precise approximations of time-minimal extremals of the Earth-Moon transfer.

4.1.3. *Time-minimal Earth-$\mathbf{L_1}$ transfer.* Set ϵ. Denoting $q = (q_1, q_2, q_3, q_4) = (x, y, \dot{x}, \dot{y})$, equations of motion in the rotating frame 17 become

$$\dot{q} = F_0(q) + \epsilon(F_1(q)u_1 + F_2(q)u_2), \;\; u_1^2 + u_2^2 \leq 1 \tag{26}$$

where

$$F_0(q) = \begin{pmatrix} q_3 \\ q_4 \\ 2q_4 + q_1 - (1-\mu)\frac{q_1+\mu}{((q_1+\mu)^2+q_2^2)^{\frac{3}{2}}} - \mu\frac{q_1-1+\mu}{((q_1-1+\mu)^2+q_2^2)^{\frac{3}{2}}} \\ -2q_3 + q_2 - (1-\mu)\frac{q_2}{((q_1+\mu)^2+q_2^2)^{\frac{3}{2}}} - \mu\frac{q_2}{((q_1-1+\mu)^2+q_2^2)^{\frac{3}{2}}} \end{pmatrix},$$

$$F_1(q) = \begin{pmatrix} 0 \\ 0 \\ 1 \\ 0 \end{pmatrix}, \;\; F_2(q) = \begin{pmatrix} 0 \\ 0 \\ 0 \\ 1 \end{pmatrix}.$$

We fix $\mu = 0.012153$ which corresponds to the gravitational constant in the Earth-Moon system. Choosing to approach the geostationary orbit by a circular one, we set q_0=(0.0947,0,0,2.8792) as the initial condition. Since the aim of the transfer is to reach the point L_1 with a zero velocity, we fix q_f=(0.8369,0,0,0) as the final condition. Hence the time-minimal transfer problem can be written

$$(\mathcal{P}_\epsilon) \begin{cases} \dot{q} = F_0(q) + \epsilon(F_1(q)u_1 + F_2(q)u_2) \\ \min_{u(.)\in B_{\mathbb{R}^2}(0,1)} \int_{t_0}^{t_f} dt \\ q(0) = q_0, \;\; q(t_f) = q_f. \end{cases} \tag{27}$$

The condition $H_r = 0$ from the maximum principle being taken into account, the corresponding shooting function is given by

$$\begin{aligned} S : \mathbb{R}^+ \times \mathbb{R}^4 &\longrightarrow \mathbb{R}^5 \\ (t_f, p_0) &\longrightarrow \begin{pmatrix} \exp_{q_0,t_f}(p_0) - q_f \\ H_r(q_f, p_f) \end{pmatrix}. \end{aligned} \tag{28}$$

where $\exp_{q_0,t_f}$ is the exponential mapping associated with H_r.The spacecraft mass is assumed to be constant and equal to 350 kg and the parameter ϵ is initialized to 1 that is a large enough value to obtain the convergence of the shooting equation. Using a simple shooting, we compute an initial extremal whose corresponding transfer time t_f and initial costate p_0 are used as the starting point of the numerical continuation. The parameter ϵ is then reduced until 0.08. These numerical values were chosen referring to the status report of ESA concerning the SMART-1 mission, see [26, 27]. At each step of the algorithm, the first conjugate time t_c^1 along the extremal is computed in order to check the necessary condition of convergence $t_c^1 > t_f$. The numerical test of conjugate times takes into account an homogeneity property in p of extremal controls, see [9], involving that the rank of the restriction of Π_q to L_t is at most 3 for each $t > 0$. So one calculates Jacobi fields $J_i(t) = (\delta q_i(t), \delta p_i(t))$ corresponding to $\delta p_i(0) = e_i$, $i = 1 \dots 4$ where $(e_i)_i$ is the canonical basis of $\mathbb{R}^4$ and one computes the rank of $(\delta q_1(t), \dots, \delta q_4(t))$ which is 3 outside a conjugate time and lower or equal to 2 at a conjugate time.

Fig. 2 and Table 1 show the time-minimal Earth-L_1 extremal trajectories in both fixed and rotating frames for $\epsilon = 1$, 0.2 and 0.08 and the comparison between the transfer time and the first conjugate time along these trajectories. According to the second order optimality condition, the time-minimal Earth-L_1 extremal trajectories we present are locally optimal. The ratio t_c^1/t_f decreases with ϵ. When $\epsilon = 1$, $t_c^1/t_f = 1.5$ and when $\epsilon = 0.08$, $t_c^1/t_f = 1.11$. We obtain a low-propulsion transfer time from the Earth to the point L_1 equal to 25.4931 units of the restricted 3-body problem, that corresponds to 110.85 days. Notice that the extremal transfers we compute are similar to transfers between Keplerian orbits when the Earth's inluence is predominant and during which the pericenter argument is constant. Futhermore, for information only, let us mention that this transfer time is approximately five times lower than the time needed during the SMART-1 mission to reach the neighborhood of L_1.

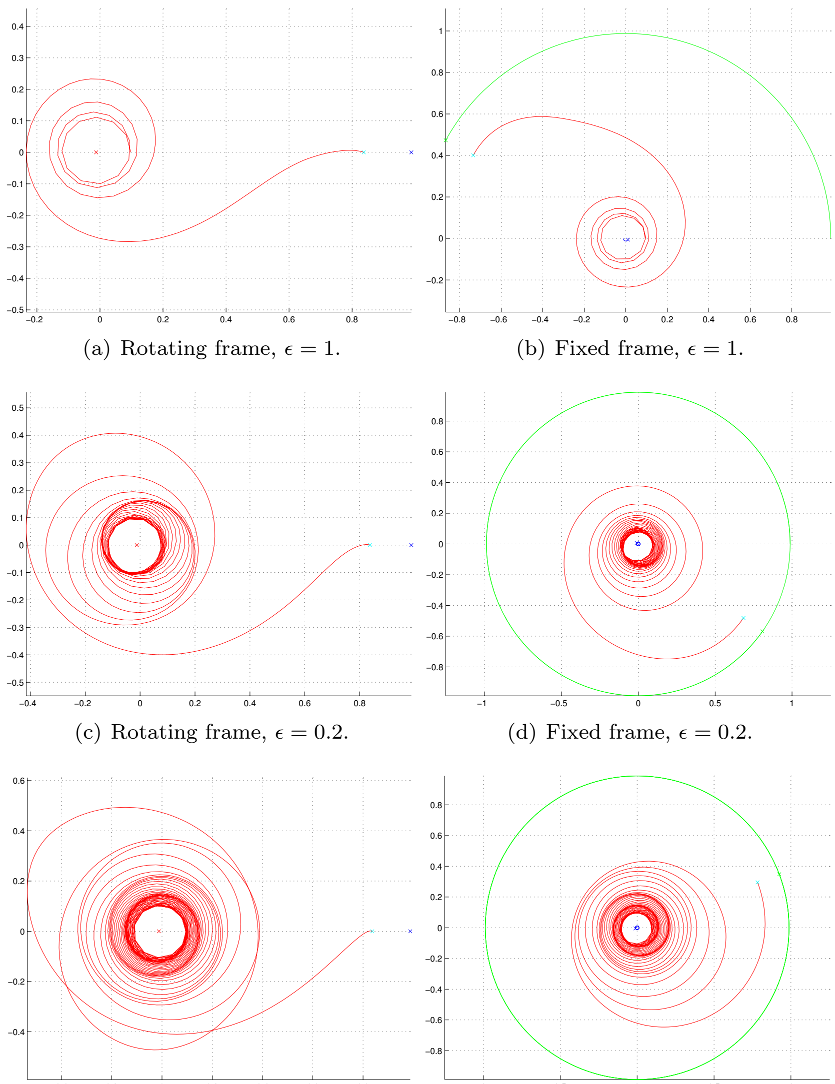

(a) Rotating frame, $\epsilon = 1$.

(b) Fixed frame, $\epsilon = 1$.

(c) Rotating frame, $\epsilon = 0.2$.

(d) Fixed frame, $\epsilon = 0.2$.

(e) Rotating frame, $\epsilon = 0.08$.

(f) Fixed frame, $\epsilon = 0.08$.

FIGURE 2. Time-minimal Earth-L_1 extremal trajectories. The red, cyan and blue crosses respectively represent the Earth, the point L_1 and the Moon. In (b), (d) and (f), the blue and green trajectories respectively correspond to Earth and Moon motion in the fixed frame.

4.1.4. *Time-minimal Earth-Moon transfer.* In this section, we consider the time-minimal transfer up to the circular orbit around the Moon $\mathcal{O}_M$ defined by

$$\mathcal{O}_M = \left\{ (q_1, q_2, q_3, q_4) \in \mathbb{R}^4, \quad \begin{array}{c} (q_1 - 1 + \mu)^2 + q_2^2 = 0.0017 \\ q_3^2 + q_4^2 = 0.2946 \\ < (q_1 - 1 + \mu, q_2), (q_3, q_4) >= 0 \end{array} \right\}.$$

ϵ	1	0.2	0.08
t_f	2.6421	11.9533	25.4931
t_c^1	3.7217	14.113	28.5194

TABLE 1. Comparision between the transfer time t_f and the first conjugate time t_c^1 (restricted 3-body problem time unit) along the time-minimal Earth-L_1 extremal trajectories.

Setting

$$h : \mathbb{R}^4 \longrightarrow \mathbb{R}^3$$
$$q \longrightarrow \begin{pmatrix} (q_1 - 1 + \mu)^2 + q_2^2 - 0.0017 \\ q_3^2 + q_4^2 - 0.2946 \\ \langle (q_1 - 1 + \mu, q_2), (q_3, q_4) \rangle \end{pmatrix}, \tag{29}$$

the time-minimal Earth-Moon transfer problem writes

$$(\mathcal{P}_\epsilon^{'}) \begin{cases} \dot{q} = F_0(q) + \epsilon(F_1(q)u_1 + F_2(q)u_2) \\ \\ \min_{u(.)\in B_{\mathbb{R}^2}(0,1)} \int_{t_0}^{t_f} dt \\ \\ q(0) = q_0, \;\; h(q(t_f)) = 0. \end{cases} \tag{30}$$

The transversality condition from the maximum principle gives $p(t_f) \perp T_{q(t_f)}\mathcal{O}_M$. The mapping h being a submersion at each point of $\mathcal{O}_M$, this condition becomes $p(t_f) \in [\text{Ker } h'(q_f)]^\perp$. The vector space Ker $h'(q_f)$ being one-dimensional, one chooses $w \in \mathbb{R}^4$ such that Ker $h'(q_f) = \text{Vect}(w)$. Hence the corresponding shooting mapping is

$$S : \mathbb{R}^+ \times \mathbb{R}^4 \longrightarrow \mathbb{R}^5$$
$$(t_f, p_0) \longrightarrow \begin{pmatrix} h(q(t_f)) \\ \langle p(t_f), w \rangle \\ H_r(q(t_f), p(t_f)) \end{pmatrix}. \tag{31}$$

The continuation algorithm is applied using the same numerical values than in the case of the Earth-L_1 transfer. However the extremal trajectory associated with $\epsilon = 1$ is computed using a simple shooting for which (t_f, p_0) is initialized with the values determined using the simple shooting method up to the point L_1. Since the target is a manifold of codimension one, the concept of conjugate time is replaced by the concept of focal time, see the definition 2.7. At each step, a backwards in time integration is proceeded to compute the first focal time t^1_{foc}. Let us consider the three-dimensional vector space spanned by Jacobi fields $J_i(t) = (\delta q_i, \delta p_i)$ for $i = 1, \ldots,\ 3$ so that $J_i(0) \in T_{(q(t_f),p(t_f))}\mathcal{O}_M^\perp$ and $\delta p_i(0)$ satisfies the normalization condition $< p(t_f), \delta p_i(0) >= 0$. The time t if a focal time if the rank of $(\delta q_1(-t), .., \delta q_4(-t))$ is strictly lower than 3.

The Earth-Moon extremal trajectories for ϵ=1, 0.2 and 0.08 in both rotating and fixed frames and the comparisons between the transfer time and the first focal time are reported on Fig.3 and on Table 2. The continuation method provides a sequence of locally time-minimal extremal trajectories. One observes that the ratio t^1_{foc}/t_f fluctuates between 2.5 and 3 which is highly superior to ratios computed in the case of the Earth-L_1 transfer. The associated low-propulsion transfer time is 26.3974 units of the restricted 3-body problem (114.78 days) that is about five times lower

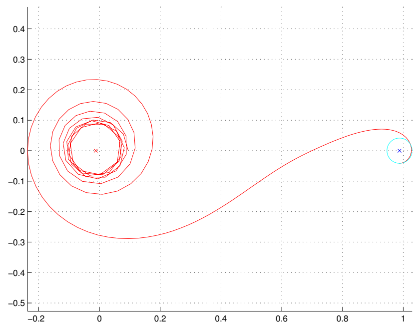

(a) Rotating frame, $\epsilon = 1$.

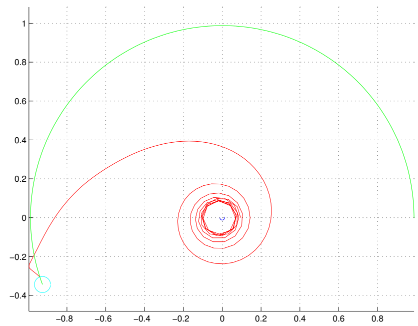

(b) Fixed frame, $\epsilon = 1$.

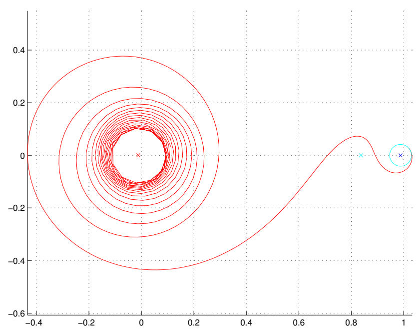

(c) Rotating frame, $\epsilon = 0.2$.

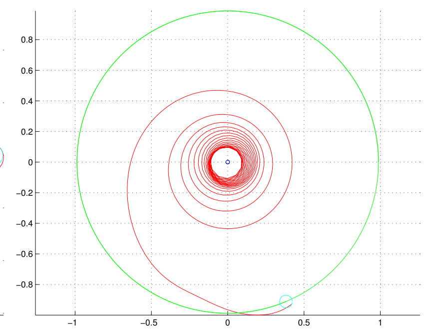

(d) Fixed frame, $\epsilon = 0.2$.

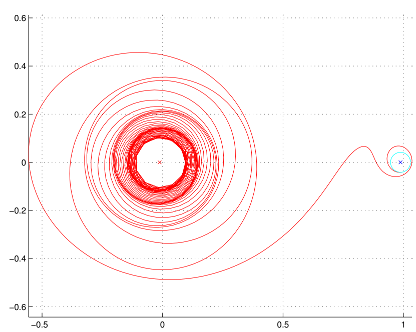

(e) Rotating frame, $\epsilon = 0.08$.

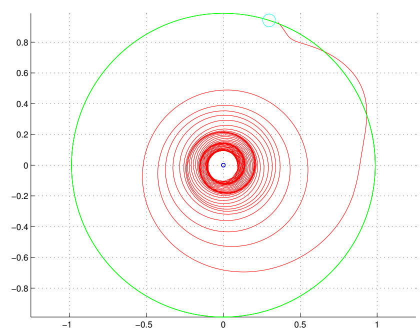

(f) Fixed frame $\epsilon = 0.08$.

FIGURE 3. Time-minimal Earth-Moon extremal trajectories. The red and blue crosses respectively represent the Earth and the Moon. The target orbit is displayed in cyan. In (b), (d) and (f), the blue and green trajectories respectively correspond to Earth and Moon motion in the fixed frame.

than the duration of the mission Smart-1. Let us remark that, as we expected, the first phases of Earth-Moon transfers are actually comparable to Earth-L_1 transfers, demonstrating the point of the Earth-L_1 transfer.

ϵ	1	0.2	0.08
t_f	3.4971	11.392	26.3974
t^1_{foc}	no focal time in $[0, 10t_f]$	28.2788	74.4602

TABLE 2. Comparision between the transfer time t_f and the first focal time t^1_{foc} (restricted 3-body problem time unit) along the time-minimal Earth-Moon extremal trajectories.

ϵ	1	0.2	0.08
t_f	2.9157	11.7107	28.1911
t^1_c	no conjugate time in $[0, 5t_f]$	no conjugate time in $[0, 5t_f]$	53.1

TABLE 3. Comparision between the transfer time t_f and the first conjugate time t^1_c (restricted 3-body problem time unit) along the time-minimal Earth-L_4 extremal trajectories.

4.1.5. *Time-minimal Earth-$\mathbf{L_4}$ transfer.* Since this problem consists in reaching the point L_4 with a zero velocity, one fixes the target $q_f = (0.4878, 0.8660, 0, 0)$. Otherwise, the corresponding optimal control problem and shooting function are the same that in the time-minimal Earth-L_1 transfer case. The continuation method we use follows exactly the same principle that the one described in the section 4.1.3. The same numerical values are employed and the conjugate time are computed using the same test. Our results are presented on 4 and Table 3.

The efficiency of the numerical continuation on the control bound ϵ is demonstrated in the context of the time-minimal Earth-L_4 transfer. Indeed, we compute a family of locally time-minimal Earth-L_4 extremal trajectories, providing a low-thrust transfer strategy. Let us notice there is no conjugate point along extremal trajectories associated with $\epsilon = 1,\ 0.2$, whereas we found a first conjugate time twice bigger than the transfer time when $\epsilon = 0.08$. These extremal trajectories are, from a topological point of view, similar to the ones we computed in the time-minimal Earth-L_1 transfer case. A progressive deformation from the circular orbit to an elliptic one that catches the point L_4 is observed. Moreover, it appears that, as in the Earth-L_1 case, the pericenter argument is constant along the transfer. The modification of the direction of the simple shooting method do not alter the topological nature of the extremal trajectories.

4.2. **Abnormal case.**

4.2.1. *Generalities in the abnormal case.* In this section, we follow the theoretical framework from [13]. First let us recall the standard method to express a bi-input system as an equivalent single-input system using a *Goh transformation.* Set $\epsilon > 0$ and consider the bi-input system

$$\dot{q} = F_0(q) + \epsilon \sum_{i=1}^{2} u_i F_i(q),\ q \in \mathbb{R}^n,\ u_1^2 + u_2^2 = 1 \tag{32}$$

with the corresponding Hamiltonian

$$H(z) = H_0(z) + u_1 H_1(z) + u_2 H_2(z). \tag{33}$$

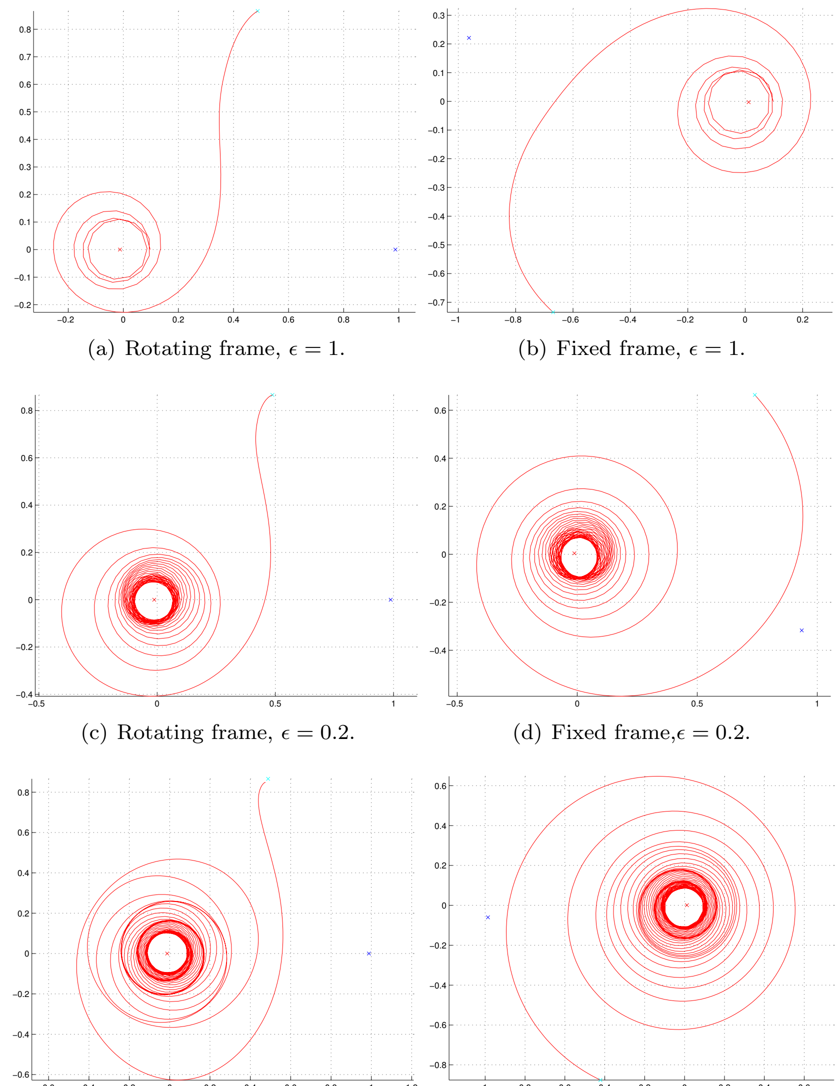

(a) Rotating frame, $\epsilon = 1$.

(b) Fixed frame, $\epsilon = 1$.

(c) Rotating frame, $\epsilon = 0.2$.

(d) Fixed frame,$\epsilon = 0.2$.

(e) Rotating frame, $\epsilon = 0.2$.

(f) Fixed frame, $\epsilon = 0.2$.

FIGURE 4. Time-minimal Earth-L_4 extremal trajectories. The red, cyan and blue crosses respectively represent the Earth, the point L_4 and the Moon.

Using the parametrization $u_1 = \cos\alpha$, $u_2 = \sin\alpha$, the equation of motion becomes

$$\dot{q} = F_0(q) + \epsilon\cos\alpha F_1(q) + \epsilon\sin\alpha F_2(q),\ \ \alpha \in \mathbb{R} \tag{34}$$

and considering the augmented variable $\widetilde{q} = (q,\ \alpha)$, one obtains the single-input system

$$\dot{\widetilde{q}} = \widetilde{F}_0(\widetilde{q}) + v\widetilde{F_1}(\widetilde{q}) \tag{35}$$

where

$$\widetilde{F}_0(\widetilde{q}) = \begin{pmatrix} F_0(q) + \epsilon\cos\alpha F_1(q) + \epsilon\sin\alpha F_2(q) \\ 0 \end{pmatrix},\ \widetilde{F}_1(\widetilde{q}) = \begin{pmatrix} 0_{\mathbb{R}^4} \\ 1 \end{pmatrix},\ v = \dot{\alpha}.$$

We have :

Theorem 4.2. *Singular extremals of the system* $(\widetilde{F}_0, \widetilde{F}_1)$ *and the control*

$$\widetilde{u}(\widetilde{z}) = -\frac{\{\{H_{\widetilde{F}_1}, H_{\widetilde{F}_0}\}, H_{\widetilde{F}_0}\}}{\{\{H_{\widetilde{F}_1}, H_{\widetilde{F}_0}\}, H_{\widetilde{F}_1}\}}$$

are the integral curves of a smooth Hamiltonian vector field $\widetilde{H}_r(\widetilde{z})$ *of the constrained space*

$$H_{\widetilde{F}_1} = \{H_{\widetilde{F}_1},\ H_{\widetilde{F}_0}\} = 0,$$

where

$$H_{\widetilde{F}_0} = <\widetilde{p}, \widetilde{F}_0>, H_{\widetilde{F}_1} = <\widetilde{p}, \widetilde{F}_1> .$$

They correspond to singular extremals of the original system.

The following proposition gives a necessary and sufficient condition for a trajectory to be locally optimal in the abnormal case.

Proposition 5. *Under generic conditions, an abnormal extremal is locally time-minimal up to the first conjugate time* t^1_{cc}.

The computation of t^1_{cc} along an abnormal extremal takes into account the condition $H_{\widetilde{F}_0} = 0$ and so differs from the computation of the first conjugate time t^1_c associated with the normal case. More precisely, one obtains the next result.

Theorem 4.3. *Along an abnormal extremal, there holds* $t_0 < t^1_{cc} < t^1_c$.

4.2.2. *Numerical study of the abnormal case.* We give a numerical illustration of the theorem 4.3 in the context of the time-minimal Earth-L_1 transfer with $\epsilon = 1$. First, we use the simple shooting method to find a zero of the shooting function

$$\begin{aligned} S : \mathbb{R}^+ \times \mathbb{R}^4 &\longrightarrow \mathbb{R}^5 \\ (t_f, p_0) &\longrightarrow \begin{pmatrix} \exp_{q_0,t_f}(p_0) - q_f \\ H_r(q_f, p_f) \end{pmatrix}. \end{aligned} \tag{36}$$

where q_0=(0.0977,0,0,0), q_f =(0.8369,0,0,0) and $\exp_{q_0,t_f}$ is the exponential mapping associated with the reduced Hamiltonian from the abnormal case

$$H_r(q,p) = H_0(q,p) + \sqrt{(H_1^2(q,p) + H_2^2(q,p))}. \tag{37}$$

We thus compute an abnormal Earth-L_1 extremal trajectory. In accordance with the theorem 4.2, this extremal corresponds to the singular extremal of the system $(\widetilde{F}_0, \widetilde{F}_1)$ defined by

$$\widetilde{F}_0(\widetilde{q}) = \begin{pmatrix} q_3 \\ q_4 \\ 2q_4 + q_1 - (1-\mu)\frac{q_1+\mu}{((q_1+\mu)^2+q_2^2)^{\frac{3}{2}}} - \mu\frac{q_1-1+\mu}{((q_1-1+\mu)^2+q_2^2)^{\frac{3}{2}}} + \cos\alpha \\ -2q_3 + q_2 - (1-\mu)\frac{q_2}{((q_1+\mu)^2+q_2^2)^{\frac{3}{2}}} - \mu\frac{q_2}{((q_1-1+\mu)^2+q_2^2)^{\frac{3}{2}}} + \sin\alpha \\ 0 \end{pmatrix},$$

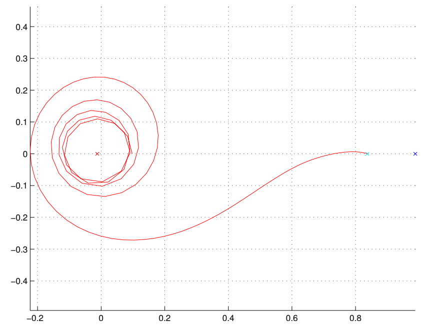

(a) Rotating frame

FIGURE 5. Time-minimal Earth-L_1 abnormal extremal trajectory, $\epsilon = 1$. The red, cyan and blue crosses respectively represent the Earth, the point L_1 and the Moon.

ϵ	t_f	t_{cc}^1	t_c^1
1	0.524	0.996	1.4

TABLE 4. Comparision between t_c^1 and t_{cc}^1 (restricted 3-body problem time unit) along the Earth-L_1 anormal extremal.

and

$$\widetilde{F}_1(\widetilde{q}) = \begin{pmatrix} 0 \\ 0 \\ 0 \\ 0 \\ 1 \end{pmatrix}.$$

whose the projection on the phase space of the initial condition is $\widetilde{q}_0 = (q_0, \alpha_0)$ where α_0 satisfies $u_1(t_0) = \cos\alpha_0$ and $u_2(t_0) = \sin\alpha_0$. Besides, the constraint $H_{\widetilde{F}_1} = 0$ involves $p_\alpha = 0$. Consequently, the augmented initial costate is given by $\widetilde{p}_0 = (p_0, 0)$. The numerical computation of the first conjugate time t_c^1 along the extremal trajectory is the same that in the normal case, see [9]. One computes the Jacobi fields corresponding to the system $(\widetilde{F}_0, \widetilde{F}_1)$ whose initial conditions $(\delta\widetilde{q}_0, \delta\widetilde{p}_0) = \delta\widetilde{z}_0$ belong to the base of the vector space determined by

$$\begin{aligned} D_{\widetilde{z}(0)}\widetilde{H}_{\widetilde{F}_1}(\delta\widetilde{z}_0) = D_{\widetilde{z}(0)}\{\widetilde{H}_{\widetilde{F}_0}, \widetilde{H}_{\widetilde{F}_1}\}(\delta\widetilde{z}_0) = 0 \\ < \widetilde{p}_0, \delta\widetilde{p}_0 >= 0 \\ \widetilde{q}_0 \in \mathbb{R}\widetilde{F}_1(\widetilde{q}_0). \end{aligned} \tag{38}$$

Since the variables of this problem are 5-dimensional, there exists three such Jacobi fields denoted $J_i(t) = (\delta\widetilde{q}_i(t), \delta\widetilde{p}_i(t))$. One then computes the first time at which $(\delta\widehat{q}_1(t), .., \delta\widehat{q}_3(t), \widetilde{F}_1(\widetilde{q}(t))) \leq 2$. The numerical computation of t_{cc}^1 follows the same principle but has to take into account the initial condition $D_{\widetilde{z}(0)}\widetilde{H}_0(\delta\widetilde{z}_0) = 0$.

The abnormal trajectory in the rotating frame and the comparison between t_{cc}^1 and t_c^1 are displayed on Fig.5 and Table 4. The expected result is checked. The specific test for abnormal extremals provides a first conjugate time strictly inferior to the one given by the test corresponding to the normal case.

5. Energy-minimal transfers in the Earth-Moon system.

5.1. Generalities. In the case of the energy-minimal transfer problem one can relax the control bound. So we consider the bi-input control system on $\mathbb{R}^n$

$$\dot{q} = F_0(q) + \sum_{i=1}^{2} u_i F_i(q), \quad u \in \mathbb{R}^2 \tag{39}$$

associated with the problem of minimizing the energy cost 21 where the time transfer t_f is fixed. The pseudo-Hamiltonian from the maximum principle is

$$H(z,u) = p^0 \sum_{i=1}^{m} u_i^2 + < p, \dot{q} > , \tag{40}$$

where $z = (q,p) \in T^*\mathbb{R}^n$ and $p^0 \le 0$. If $p^0 < 0$ one can, using homogeneity, normalize p^0 to -1/2. From the maximization condition $\partial H/\partial u$ =0, one deduces that

$$u_i = H_i(z) =< p, F_i(q) >, \; i = 1, \; 2. \tag{41}$$

Substituting, one gets the true Hamiltonian

$$H_r(z) = H_0(z) + \frac{1}{2} \sum H_i^2(z). \tag{42}$$

5.2. The continuation method on the gravitational constant. The mathematical continuation method in the restricted circular problem was used by Poincaré, in particular for the continuation of circular orbits. Geometrically, it is simply a continuation of trajectories of the Kepler problem into trajectories of the 3-body problem. It amounts to consider μ as a small parameter, the limit case $\mu = 0$ being Kepler problem in the rotating frame, writing

$$H_0 = \frac{\| p \|^2}{2} - {}^t qKp - \frac{1}{\| q \|} + o(\mu) \tag{43}$$

and the approximation for μ is valid, a neighborhood of the primaries being excluded. In the Earth-Moon problem, since μ is very small, the Kepler problem is clearly a good approximation of the motion in a large neighborhood of the Earth. This point of view is important in our analysis, as indicated by the status report of the SMART-1 mission since most of the time mission is under the influence only of the Earth attraction, see [26, 27].

5.3. Energy-minimal Earth-$\mathbf{L_1}$ transfer. Firstly we chose to simulate the energy-minimal Earth-L_1 transfer in the restricted 3-body problem. Indeed, when $\mu = 0$, the Moon and the point L_1 are identical. Furthermore, in the Earth-Moon system, the point L_1 and the Moon are located very closely, which suggests that the first phase of the Earth-Moon transfer is comparable, as in the time-minimal Earth-Moon transfer, to the Earth-L_1 transfer. Retaining the notations of the section 4, the energy-minimal Earth-L_1 transfer problem, parametrized with μ and the transfer time t_f, can be written

$$(\mathcal{P}_\mu) \begin{cases} \dot{q} = F_0(q) + F_1(q)u_1 + F_2(q)u_2 \\ \\ \min_{u(.) \in \mathbb{R}^2} \int_{t_0}^{t_f} u_1^2 + u_2^2 dt \\ \\ q(0) = q_0, \;\; q(t_f) = q_f \end{cases} \tag{44}$$

μ	0	0.012153
t_f	121	121
t_c^1	no focal time in $[0, 5t_f]$	121.932

TABLE 5. Comparision between the transfer time t_f and the first conjugate time t_c^1 (restricted 3-body problem time unit) along the energy-minimal Earth-Moon extremal trajectories.

which leads to solve the shooting equation associated with the mapping

$$\begin{aligned} S : \mathbb{R}^4 &\longrightarrow \mathbb{R}^4 \\ p_0 &\longrightarrow \exp_{q_0,t_f}(p_0) - q_f. \end{aligned} \tag{45}$$

By making the parameter μ vary from 0 to 0.012153, one builds up a family $(S_\mu)_\mu$ of shooting functions which connects both Kepler and restricted 3-body problem. The continuation method may then be used to deduce an Earth-L_1 transfer with low-thrust from Keplerian trajectories. The following results that we present are obtained setting q_0=(0.0977,0,0,2.8792) as the initial condition.Referring to the status report of the SMART-1 mission, see [26, 27], we fix the transfer time to 121 units of the restricted 3-body problem (526.1365 days) and the spacecraft mass is assumed to be constant to 350kg. Setting $\mu = 0$, we compute an initial extremal using a simple shooting. Then we make the parameter μ vary up to 0.012153. Since t_f is fixed, the domain of $\exp_{x_0,t_c}$ is locally diffeomorphic to $\mathbb{R}^4$, see [9]. Consequently one determines the first conjugate time by computing the Jacobi fields $J_i(t) = (\delta x_i(t), \delta p_i(t)),\ i = 1, \ldots,\ 4$, corresponding to initial conditions $\delta x_i(0) = 0$ and $\delta p_i(0) = e_i$, where $(e_i)_i$ is the canonical basis of $\mathbb{R}^4$. Then $\mathrm{rank}(\delta x_1(t), .., \delta x_4(t))$ is equal to 4 outside a conjugate time and lower or equal to 3 at a conjugate time. Moreover we plot the Euclidean norm of extremal controls to compare the control bound and the maximal thrust allowed by electro-ionic engines.

Fig.6 and Table 5 show extremal trajectories in both rotating and fixed frames, the Euclidean norm of extremal controls and the comparisons between the transfer time and the first conjugate time in the Kepler problem and the restricted 3-body problem. The numerical continuation on μ provides an energy minimal Earth-L_1 extremal trajectory resulting from the distortion of a Keplerian one, in accordance with Poincaré's theory. This transfer consists in joining an elliptic orbit around the Earth from the geostationary one by preserving the pericenter argument, before reaching the point L_1. The second order optimality condition ensures that the extremals are locally optimal in $L^\infty([0, t_f])$. One can notice that in both cases $\mu = 0$ and $\mu = 0.012153$, the maximum value reached by the norm of the extremal control is approximately twice inferior to the low-thrust bound $\epsilon \leq 0.08$ (0.073 N), but the transfer times are roughly the same.

5.4. **Energy-minimal Earth-Moon transfer.** Conserving the definition of the circular orbit around the Moon $\mathcal{O}_M$, the energy-minimization Earth-Moon transfer

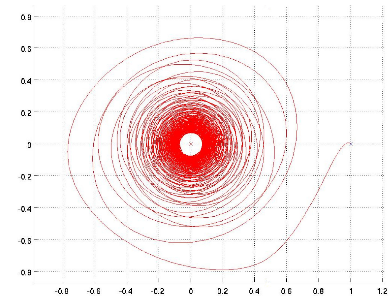

(a) Rotating frame, $\mu = 0$.

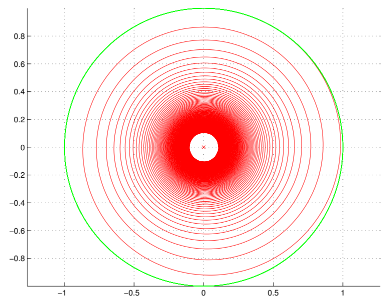

(b) Fixed frame, $\mu = 0$.

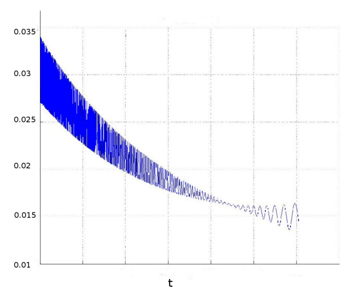

(c) Norm of the extremal control along the transfer, $\mu = 0$.

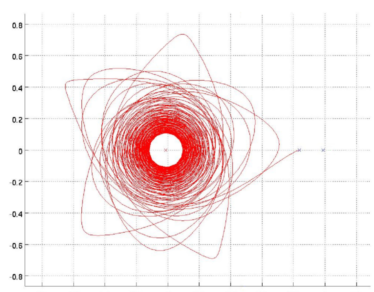

(d) Rotating frame, $\mu = 0.012153$.

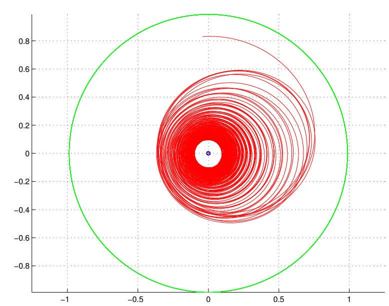

(e) Fixed frame, $\mu = 0.012153$.

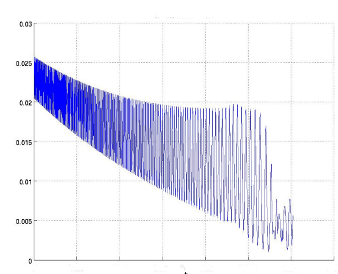

(f) Norm of the extremal control along the transfer, $\mu = 0.012153$.

FIGURE 6. Energy-minimal Earth-L_1 extremal trajectories. The red cross represents the Earth. In (b), the green trajectory corresponds to motion of the point L_1 which is identical to the Moon. In (d) and (e), the point L_1 and the Moon are different and respectively represented by cyan and blue crosses. The green trajectory correspond to the Moon motion in the fixed frame.

μ	1	0.2
t_f	124	124
t^1_{foc}	192.5432	212.5761

TABLE 6. Comparision between the transfer time t_f and the first focal time t^1_{foc} (restricted 3-body problem time unit) along the energy-minimal Earth-Moon extremal trajectories.

problem can be written

$$(\mathcal{P}'_\mu) \begin{cases} \dot{q} = F_0(q) + F_1(q)u_1 + F_2(q)u_2 \\ \min_{u(.)} \int_{t_0}^{t_f} u_1^2 + u_2^2 dt \\ q(0) = q_0, \;\; h(q(t_f)) = 0. \end{cases} \tag{46}$$

where h is the mapping defined in 29. The transfer time t_f is fixed and the shooting function S becomes

$$\begin{aligned} S : \mathbb{R}^4 &\longrightarrow \mathbb{R}^4 \\ p_0 &\longrightarrow \begin{pmatrix} (q_1 - 1 + \mu)^2 + q_2^2 - 0.0017 \\ q_3^2 + q_4^2 - 0.2946 \\ < (q_1 - 1 + \mu, q_2), (q_3, q_4) > \\ < p(t_f), w > \end{pmatrix}. \end{aligned} \tag{47}$$

The transfer time is set to 124 time units of the restricted 3-body problem (539.18 days) and the spacecraft mass remains constant and equal to 350 kg. An extremal corresponding to $\mu = 0$ is computed using a simple shooting method, the initial costate p_0 being initialized with the one associated with the energy-minimal Earth-L_1 transfer. The method to compute the first focal time has to take into account the fixed value of the transfer time, see [9]. Hence the normalization condition $< p(t_f), \delta p_i(0) >= 0$ does not hold anymore. One considers the 4-dimensional vector space spanned by th Jacobi fields $J_i(t) = (\delta x_i, \delta p_i)$, $i = 1, .., 4$, satisfying $J_i(0) \in T_{z(t_f)}\mathcal{O}_M^\perp$. At time t one computes $\text{rank}(\delta x_1(-t), .., \delta x_4(-t))$ which is inferior or equal to 3 at a focal time and equal to 4 outside a focal time. We thus compute a locally energy-minimizing Earth-Moon trajectory. In both cases $\mu = 0$ and $\mu = 0.012153$, the first focal time along extremal is superior to $3/2t_f$. The control bound is approximately 0.045, which corresponds to the half of the maximal thrust allowed by the SMART-1 low-propulsion engines. An interesting remark is that, when $\mu = 0$, the Keplerian Earth-L_1 trajectory significantly differs from the Keplerian Earth-Moon trajectory. This difference illustrates the effect of the transversality condition when the final target is a submanifold. On the contrary, when $\mu = 0.012153$ the first phase of the Earth-Moon transfer is comparable to the Earth-L_1 transfer. This underlines the crucial role of the neighborhood of the point L_1 where the attractions of the two primaries compensate each other.

The Earth-Moon trajectories in both rotating and fixed frame, the norm of the extremal controls the comparison between the first focal time and the transfer time are shown on Fig.7 and Table 6, for $\mu = 0$ and $\mu = 0012153$.

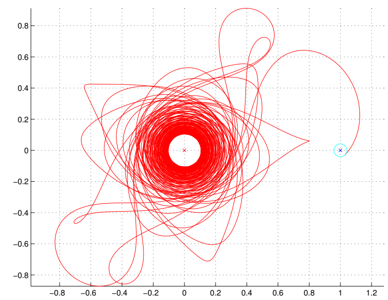

(a) Rotating frame, $\mu = 0$.

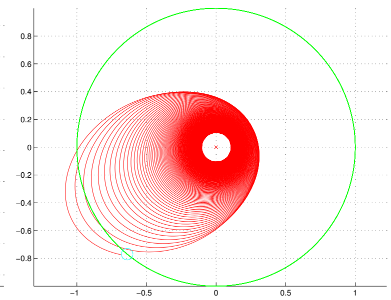

(b) Fixed frame, $\mu = 0$.

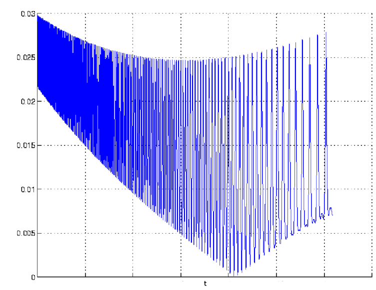

(c) Norm of the extremal control along the transfer, $\mu = 0$.

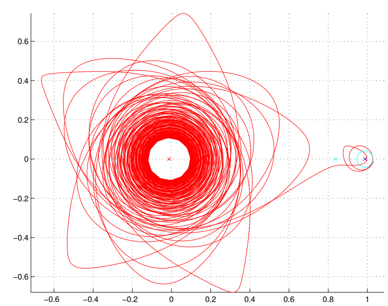

(d) Rotating frame, $\mu = 0.012153$.

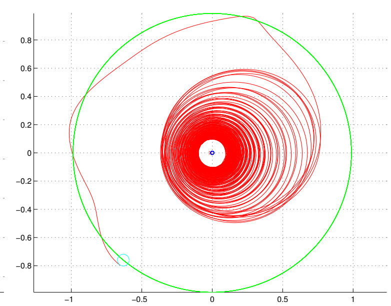

(e) Fixed frame, $\mu = 0.012153$.

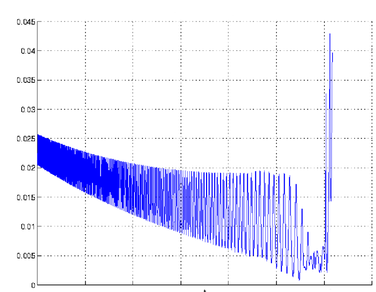

(f) Norm of the extremal control along the transfer, $\mu = 0.012153$.

FIGURE 7. Energy-minimal Earth-Moon extremal trajectories. The red and blue crosses respectively represent the Earth and the Moon. The cyan circle is the target orbit. In (b) and (e), the blue and green trajectories respectively correspond to Earth and Moon motion in the fixed frame.

6. **Conclusion.** The main contribution of this article is to provide two large sets of time-minimal and energy-minimal spatial trajectories inside the Earth-Moon system, considered as solution of the controlled restricted 3-body problem, in a context of low-thrust. In particular, we estimate the time optimal low-energy transfer between the geostationary orbit and a circular parking orbit around the Moon. We also provide a numerical checking of the comparison theorem between the first conjugate times in normal and abnormal cases related to the time-minimal problem. Moreover, by giving an estimation of the energy minimizing trajectory beetwen the same orbits, we suggest a starting point for the homotopy method which relates the energy minimization problem and the final spacecraft mass problem. Our computations result from an original application of indirect numeric methods, inspired by the Pontryagin maximum principle, to the particular planar restricted 3-body problem and the optimality of these transfers is checked using second order conditions. The efficiency of such a process is well-known for strongly depending on determining accurate initial conditions, which is performed thanks to relevant continuation methods, founded on numeric, in the time-minimal case, or physical, in the energy-minimal case, considerations. Furthermore, this work underlines the crucial role played by the Lagrangian point L_1 by verifying that the first phase of an optimal Earth-Moon trajectory is similar to an Earth-L_1 transfer, that is comparable to a transfer between Keplerian orbits in the Earth's gravity area during which the pericenter argument is constant. This encourages future studies dealing with the link between the invariant manifolds in the neighborhood of L_1 and optimal transfers in the restricted 3-body problem. In addition, we give some important qualitative observations about extremal of the restricted 3-body problem since it appears that the topological caracteristics of time-minimal extremal trajectories are preserved when the transfer's target is modified, as we noticed by comparing transfers up to the points L_1 and L_4.

Acknowledgments. The author thanks Pr. B. Bonnard and Pr. J.B. Caillau from the Mathematics Institute of the Bourgogne University for many advices and helpfull discussions.

REFERENCES

[1] A.A. Agrachev and A.V. Sarychev, *On abnormals extremals for Lagrange variational problem*, J. Math. Systems. Estim. Control , **1** (1998), 87–118.

[2] E.L Allgower and K. Georg, "Numerical Continuation Methods, An Introduction", Springer, Berlin, 1990.

[3] V. I. Arnold, "Mathematical Methods of Classical Mechanics", Springer, New-York, 1989.

[4] J.T. Betts and S.O. Erb, *Optimal low thrust trajectories to the Moon*, SIAM J. Appl. Dyn. Syst., **2** (2003), 144–170.

[5] C. Bischof, A. Carle, P. Kladem and A. Mauer, *Adifor 2.0: Automatic Differentiation of Fortran 77 programs.* , IEEE Computational Science and Engineering, **3,(3)** (1996), 18–32.

[6] G. A. Bliss, "Lectures on the Calculus of Variations", Chicago, 1946.

[7] A. Bombrun, J.Chetboun and J-B Pomet, *Transfert Terre-Lune en poussée faible par contrôle feedback – La mission SMART-1*, (French) INRIA Research report, **5955** (2006), 1–27.

[8] B. Bonnard, J.B. Caillau and G. Picot, *Geometric and numerical techniques in optimal control of the two and three body problems*, Commun. Inf. Syst., **4** (2010), 239–278.

[9] B. Bonnard, J.-B. Caillau and E. Trélat, *Second order optimality conditions in the smooth case and applications in optimal control*, ESAIM Control Optim. and Calc. Var., **2** (2007), 207–236.

[10] B. Bonnard, J.-B. Caillau and E. Trélat, *COTCOT: short reference manual*, ENSEEIHT-IRIT Technical report RT/APO/05/1, (2005), 1–15.

[11] B. Bonnard and M. Chyba, "Singular Trajectories and Their Role in Control Theory", Math. and Applications 40, Springer, 2003.

[12] B. Bonnard, L. Faubourg and E. Trélat, "Mécanique Céleste et Contôle des Véhicules Spatiaux", Springer-Verlag, Berlin, 2006.

[13] B. Bonnard and I. Kupka, *Théorie des singularités de l'application entrée/sortie et optimalité des trajectoires singulières dans le problème du temps minimal*, (French)[Theory of the singularities of the input/output mapping and optimality of singular trajectories in the minimal-time problem], Forum Math., **2** (1998), 111–159.

[14] B. Bonnard, N. Shcherbakova and D. Sugny, *The smooth continuation method in optimal control with an application to quantum systems*, ESAIM Control Optim. and Calc. Var., **1** (2011), 267–292.

[15] J.-B. Caillau, "Contribution à l'Etude du Contrôle en Temps Minimal des Transferts Orbitaux", Ph.D thesis, Toulouse University, 2000.

[16] J.-B. Caillau, B. Daoud and J. Gergaud, *On some Riemannian aspects of two and three-body controlled problems*, in "Recent Advances in Optimization and its Applications in Engineering" , Springer, (2010), 205–224.

[17] J.-B. Caillau, B. Daoud and J. Gergaud, *Discrete and differential homotopy in circular restricted three-body control*, in "AIMS Proceedings", (2010), to appear.

[18] J. Gergaud and T. Haberkorn, *Homotopy method for minimum consumption orbit transfer problem*, ESAIM Control Optim. Calc. Var., **12** (2006), 294–310.

[19] G. Gómez, S.Koon, M. Lo, J.E Marsden, J. Masdemont and S.D. Ross, *Invariant manifolds, the spatial three-body problem ans space mission design*, in "the proceedings of AIAA/AAS Astrodynamics Specialist Meeting, Quebec City, Quebec, Canada", (2001).

[20] M. Guerra and A. Sarychev, *Existence and Lipschitzian regularity for relaxed minimizers*, in "Mathematical control theory and finance", Springer, Berlin 2008, 231–250.

[21] J.E. Marsden and S.D. Ross, *New methods in celestial mechanics and mission design*, Bull. Amer. Math. Soc. (N.S), **1** (2006), 43–73.

[22] K. Meyer and G. R. Hall, "Introduction to Hamiltonian Dynamical Systems and the N-Body Problem", Springer, New York, 1992.

[23] H. Poincaré, "Oeuvres", Gauthier-Villars, Paris, 1934.

[24] H. Pollard, "Mathematical Introduction to Celestial Mechanics", Prentice-Hall, Englewood Cliffs, 1966.

[25] L. S. Pontryagin, V. G. Boltyanskii, R. V. Gamkrelidze and E. F. Mishchenko, "The Mathematical Theory of Optimal Processes", John Wiley & Sons, New York, 1962.

[26] G. Racca, B. H. Foing and M. Coradini, *SMART-1: The first time of Europe to the Moon*, Earth, Moon and planets, **85-86** (2001), 379–390.

[27] G. Racca et al., *SMART-1 mission description and development status*, Planetary and space science, **50** (2002), 1323–1337.

[28] A.V. Sarychev, *Index of second variation of a control system*, Mat. Sb. (N.S), **113** (1980), 464–486.

[29] L.F. Shampine, H.A. Watts and S. Davenport, *Solving non-stiff ordinary differential equations-the state of the art.*, SIAM Rev., **3** (1976), 376–411.

[30] V. Szebehely, "Theory of Orbits: The Restricted Problem of Three Bodies", Academic Press, 1967.

Received xxxx 20xx; revised xxxx 20xx.

E-mail address: gautier.picot@u-bourgogne.fr